

Theory of transport properties of the sixfold-degenerate two-dimensional electron gas at the H-Si(111) surface

A. Gold

Centre d'Elaboration de Matériaux et d'Etudes Structurales (CEMES), CNRS, 29 Rue Jeanne Marvig, 31055 Toulouse, France and UFR-PCA, Université Paul Sabatier, 31062 Toulouse, 118 Route de Narbonne, France

(Received 21 May 2010; revised manuscript received 30 October 2010; published 24 November 2010)

We consider the mobility of the interacting two-dimensional electron gas as realized at the hydrogen terminated Si(111) surface with sixfold valley degeneracy. For zero temperature we calculate the mobility as function of the electron density for charged-impurity scattering. We take into account many-body effects. Multiple-scattering effects, leading to a metal-insulator transition at low electron density, are also taken into account. Our calculation is in agreement with recent experimental results. We also present analytical results for the mobility and we study the importance of interface-roughness scattering. For the spin-polarized electron gas, created by applying a parallel magnetic field, we predict the mobility and the phase diagram of the metal-insulator transition.

DOI: [10.1103/PhysRevB.82.195329](https://doi.org/10.1103/PhysRevB.82.195329)

PACS number(s): 73.20.Fz, 73.50.Bk, 73.61.Cw, 73.43.Qt

The two-dimensional electron gas (2DEG) at the surface of Si(111) should have a valley degeneracy $g_v=6$.¹ Early experimental studies of transport properties showed that $g_v=2$, for a review see Ref. 1, but also $g_v=6$ was reported.² During the passed five years the study of the mobility and the valley degeneracy of the 2DEG at the Si(111) interface has got new interest, in connection with the existence of a metal-insulator transition (MIT) (Refs. 3 and 4) and very high mobility samples.⁵⁻⁷ For instance, at low temperature the magnetoresistance in a parallel magnetic field was measured for a low mobility sample.³ A MIT at a critical density $N_{\text{MIT}} \approx 3 \times 10^{11} \text{ cm}^{-2}$ in a $g_v=2$ Si(111) was reported using a metal-oxide-semiconductor field-effect transistor (MOSFET) for a sample with a peak mobility, at low temperatures, of $\mu_{\text{peak}} \approx 2.5 \times 10^3 \text{ cm}^2/\text{Vs}$.⁴ Recently grown samples,⁵⁻⁷ made with hydrogen-passivated Si(111)/vacuum [H-Si(111)] structures, had higher mobility $\mu \approx 2.4 \times 10^4 \text{ cm}^2/\text{Vs}$ with $g_v=2$ at low electron density and with $g_v=6$ at high electron density.⁶ Very recently a still higher mobility $\mu \approx 10^5 \text{ cm}^2/\text{Vs}$ together with a MIT at $N_{\text{MIT}} \approx 0.9 \times 10^{11} \text{ cm}^{-2}$ and a valley degeneracy $g_v=6$ was found with H-Si(111) samples.⁷ The mobility versus density data of Ref. 7, determined at the very low temperature 70 mK, are discussed in the present paper. We expect that our results will initiate additional experiments with such H-Si(111) structures.

The transport properties of the electron gas in Si(111) MOSFET structures near the MIT, as observed in Ref. 4, have been analyzed from a theoretical point of view in great detail.⁸ The key point was to introduce a density-dependent effective mass as observed in experiment. More generally, from theory it was argued that due to improved screening properties of the 2DEG due to the high valley degeneracy the mobility in Si(111) should be much larger than in the corresponding 2DEG at the Si(100) surface with $g_v=2$.⁹ In fact, by analyzing magnetoresistance data from Ref. 3 it was concluded that in the Si(111) MOSFET structure used there the valley degeneracy was $g_v=2$.⁹ Transport data in H-Si(111) from Ref. 5 already have been analyzed¹⁰ within a two-subband model as proposed in Ref. 6. From the theoretical

results in Refs. 9 and 10 it is obvious that in the 2DEG at the H-Si(111) surface a MIT occurs at low electron density¹¹ and that the mobility in this system should be very high due to the large valley degeneracy.

For zero temperature a transport theory for the 2DEG in Si(100) MOSFET structures, including a MIT at low electron density, was proposed some time ago and found in good agreement with experiments.^{12,13} In the present paper we use this mode-coupling approach for $g_v=6$ in order to treat multiple-scattering effects (MSE). We consider an interacting 2DEG in the xy plane with parabolic dispersion and effective isotropic mass $m^*=0.358m_e$ in the plane of the electron gas and with a perpendicular mass $m_z=0.258m_e$.¹ m_e is the free electron mass. The valley degeneracy is assumed to be $g_v=6$. The electron gas at the surface of Si(111) is embedded into an isolating background of effective dielectric constant $\epsilon_L=6.25$, which is the mean value between of the dielectric constant of Si $\epsilon_{\text{Si}}=11.5$ and the vacuum $\epsilon_{\text{vac}}=1$. The interaction effects of the 2DEG are treated using the random-phase approximation (RPA) (Refs. 1 and 14) together with a finite local-field correction (LFC).¹⁵ Extension effects of the electron gas perpendicular to the interface are described by a triangular potential well with the confinement parameter b for the wave function $\Psi(z>0) \propto z \exp(-bz)$, for which we use the Howard-Stern expression¹ with depletion density $N_{\text{depl}}=1 \times 10^{11} \text{ cm}^{-2}$. The electron gas is strongly correlated because of the large Wigner-Seitz parameter $r_s \equiv 1/\sqrt{\pi a^* N}$ at low density. $a^* \equiv 0.53 \text{ \AA} \epsilon_L m_e/m^* = 9.24 \text{ \AA}$ represents the effective Bohr radius. For $N=1 \times 10^{12} \text{ cm}^{-2}$ the Wigner-Seitz parameter takes the large value $r_s \approx 6.1$. The LFC $G(q)$ describes many-body effects (exchange and correlation) beyond the RPA and these effects become important for low electron density ($r_s > 1$, $N < 3.73 \times 10^{13} \text{ cm}^{-2}$). We use in this paper analytical expressions of the LFC according to the numerical results obtained as in Ref. 16, however for $g_v=6$.

We study the transport properties of the 2DEG in the presence of impurity scattering. The scattering mechanism is parameterized as for silicon MOSFET structures.^{1,13,17} We assume charged impurities at the interface vacuum/silicon with an impurity density N_i . We also discuss interface-roughness

scattering, which is characterized by the length parameters Δ and Λ . The length Δ represents the average height of the roughness perpendicular to the 2DEG and Λ represents the correlation-length parameter of the roughness in the xy plane of the 2DEG. We shall show that for the electron densities probed in the experiment of Ref. 7 interface-roughness scattering can be neglected.

For the mobility calculated in lowest order of the disorder (the random potential $\langle |U(\vec{q})|^2 \rangle$) we use the symbol μ_0 . The mobility is given in terms of the transport scattering time $\tau_t^{(0)}$ via $\mu_0 = e\tau_t^{(0)}/m^*$. The inverse transport scattering time $\tau_t^{(0)}$ is expressed as^{1,13}

$$\frac{\hbar}{\tau_t^{(0)}} = \frac{1}{2\pi\epsilon_F} \int_0^{2k_F} dq \frac{q^2}{\sqrt{4k_F^2 - q^2}} \frac{\langle |U(\vec{q})|^2 \rangle}{\epsilon(q)^2} \quad (1)$$

ϵ_F represents the Fermi energy, k_F the Fermi wave number, and $\epsilon(q)$ is the dielectric function including the LFC. When MSE (Ref. 13) are taken into account we use for the mobility the symbol μ . MSE are very important at low electron density and are the origin for the MIT at N_{MIT} . For $N > N_{\text{MIT}}$ the mobility can be written¹⁷ as

$$\mu = \mu_0(1 - A) \quad (2)$$

with $A \leq 1$. The parameter A describes MSE and depends on the random potential, the screening function, and the compressibility of the electron gas.¹³ The MIT at N_{MIT} is defined by $A=1$. For $N < N_{\text{MIT}}$ the mobility vanishes: $\mu=0$. For given parameters of the disorder (N_i) the theory predicts N_{MIT} depending on N_i and the spin degeneracy g_s . With the approximation $A \approx N_{\text{MIT}}/N$ the mobility is written as $\mu_{fit} = \mu_0(1 - \frac{N_{\text{MIT}}}{N})$ for $N > N_{\text{MIT}}$ and by $\mu_{fit}=0$ for $N < N_{\text{MIT}}$. μ_{fit} interpolates between $\mu_{fit}=0$ for $N \leq N_{\text{MIT}}$ and $\mu_{fit}=\mu_0$ for $N \gg N_{\text{MIT}}$. For N_{MIT} it is difficult to get perfect agreement between theory and experiment. Therefore, for the comparison of μ_{fit} with experimental results we take the critical density N_{MIT} from experiment and choose N_i such to get agreement with the experimental mobility data at higher electron density.

We mention that in the mode-coupling approach weak-localization effects are neglected. It was shown in experiments, using the 2DEG, that weak-localization effects don't lead to a MIT.¹⁸ For a recent review concerning the MIT in the 2DEG see Ref. 19. However, we stress that the existence of a MIT in 2DEG is an experimental fact, as already discussed long ago in Ref. 1.

With a parallel magnetic field the 2DEG becomes spin polarized.²⁰ We suppose that one can neglect orbital effects and that only spin effects are important. In this case the resistance of the electron gas increases as function of the parallel magnetic field and becomes constant for $B \geq B_c$.²¹ B_c is the magnetic field for complete spin polarization.²⁰ The spin degeneracy of a completely spin-polarized electron gas is $g_s=1$. The screening properties of the spin-polarized electron gas are reduced and the resistance is larger than for a nonpolarized electron gas with $g_s=2$. For the MIT this leads to $N_{\text{MIT}}^{g_s=1} > N_{\text{MIT}}^{g_s=2}$, which means that if the magnetoresistance

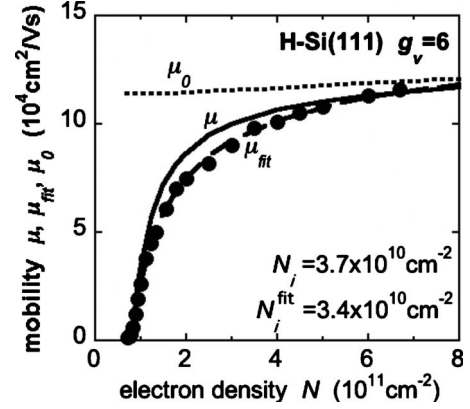


FIG. 1. Mobility μ_0 and μ versus electron density N of the electron gas at the H-Si(111) interface for charged-impurity scattering with $N_i=3.7 \times 10^{10} \text{ cm}^{-2}$ as the dotted and solid line, respectively. The dashed line represents μ_{fit} with $N_i=3.4 \times 10^{10} \text{ cm}^{-2}$. The solid dots represent experimental results of Ref. 7.

ratio $\rho(B_c)/\rho(B=0) \equiv \mu(g_s=2)/\mu(g_s=1)$ versus density is considered one finds a divergent behavior when approaching $N_{\text{MIT}}^{g_s=1}$.²²

Due to anomalous screening²³ in two dimensions the mobility of the 2DEG shows a linear temperature dependence, written as²⁴

$$\mu_0(T) = \mu_0 \left(1 - C(\alpha, N) \frac{k_B T}{\epsilon_F} + O(T^{3/2}) \right). \quad (3)$$

The coefficient $C(\alpha, N)$ depends on the scattering mechanism (α), the electron density, the LFC and the form factors for extension effects of the 2DEG.²⁵ For given electron density the Fermi energy is small if the valley degeneracy is large. This leads, for given N , to a three times larger value of $1/\epsilon_F$ for Si(111) compared to Si(100).

In Fig. 1 we show the mobility for impurity scattering versus electron density. The impurity density at the interface was chosen as $N_i=3.7 \times 10^{10} \text{ cm}^{-2}$. The dotted line represents the mobility μ_0 in lowest order and μ_0 is nearly constant with increasing electron density. The solid line represents the mobility μ including MSE and a MIT occurs at $N_{\text{MIT}}=N_{\text{MIT}}^{g_s=2}=7.94 \times 10^{10} \text{ cm}^{-2}$. Good agreement within 10% is obtained in comparison with the experimental results of Ref. 7 shown as the solid dots. The dashed line represents μ_{fit} with $N_i=3.4 \times 10^{10} \text{ cm}^{-2}$ and $N_{\text{MIT}}=7.94 \times 10^{10} \text{ cm}^{-2}$. The very good agreement of the dashed line with the data points shows that the mobility is very nicely described by N_{MIT} and μ_0 .

The fact that, for given electron density, an increasing valley degeneracy increases the mobility $\mu_0(N \rightarrow 0) \propto \tau_t^{(0)}(N \rightarrow 0) \propto g_v^2/N_i$ was already shown long ago, see Eq. (15) in Ref. 25. It means that Si(111) with $g_v=6$ should have, for the same electron density, a nine times larger transport scattering time than Si(100). We note that for given electron density the Fermi wave number for the 2DEG is smaller in Si(111) than in Si(100), which means that form factors for the mobility are less important, which gives rise, for low density, to a nearly density independent mobility. The large density de-

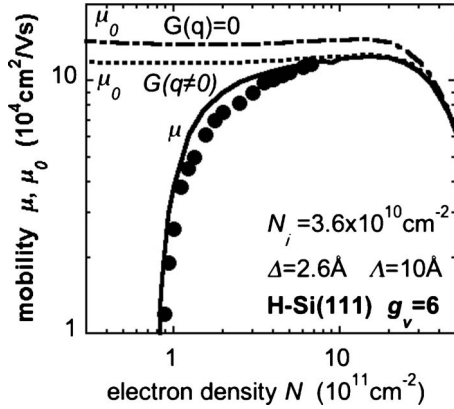


FIG. 2. Mobility μ_0 and μ versus electron density N of the two-dimensional electron gas at the H-Si(111) interface for charged-impurity scattering with $N_i = 3.6 \times 10^{10} \text{ cm}^{-2}$ and interface-roughness scattering with $\Delta = 2.6 \text{ \AA}$ and $\Lambda = 10 \text{ \AA}$ as the dotted and solid line, respectively. The dashed-dotted line represents μ_0 , where many-body effects described by the LFC are neglected. The solid dots represent experimental results of Ref. 7.

pendence of the mobility seen in experiment, see Fig. 1, can be described by MSE. This is an extremely important point: the lowest order result is nearly independent on density.

In Fig. 2 we again show the mobility versus density in comparison with experimental results,⁷ however in a larger density range. Charged-impurity scattering and interface-roughness scattering is taken into account. We use $N_i = 3.6 \times 10^{10} \text{ cm}^{-2}$, $\Delta = 2.6 \text{ \AA}$, and $\Lambda = 10 \text{ \AA}$. For the solid line MSE are taken into account. For the dotted line MSE are neglected. It is clear that due to missing data at high electron density we cannot really get information about interface-roughness scattering. But we conclude from the results shown in Fig. 2 that interface-roughness scattering is not very important for the sample and the density range studied in Ref. 7. The dashed-dotted line represents μ_0 within the RPA where many-body effects are neglected. It is higher by 50% compared to the calculation within lowest order with the LFC taken into account.

For the nonpolarized and spin-polarized electron gas we have studied the density $N_{\text{MIT}}^{g_s}$ of the MIT numerically. For $N > N_{\text{MIT}}$ the system is metallic, for $N < N_{\text{MIT}}$ an insulating phase is found. With increasing impurity density the critical density N_{MIT} increases. In the density range $10^{10} \text{ cm}^{-2} < N_{\text{MIT}}^{g_s} < 10^{12} \text{ cm}^{-2}$ we find the relations $N_{\text{MIT}}^{g_s=2}/10^{11} \text{ cm}^{-2} \cong 1.52 \times (N_i/10^{11} \text{ cm}^{-2})^{0.65}$ and $N_{\text{MIT}}^{g_s=1}/10^{11} \text{ cm}^{-2} \cong 1.85 \times (N_i/10^{11} \text{ cm}^{-2})^{0.62}$ and we conclude that $N_{\text{MIT}}^{g_s=1} > N_{\text{MIT}}^{g_s=2}$ for given N_i .²² For $N_i = 3.7 \times 10^{10} \text{ cm}^{-2}$ we find numerically $N_{\text{MIT}}^{g_s=2} = 7.94 \times 10^{10} \text{ cm}^{-2}$ and $N_{\text{MIT}}^{g_s=1} = 10.2 \times 10^{10} \text{ cm}^{-2}$ with $N_{\text{MIT}}^{g_s=1}/N_{\text{MIT}}^{g_s=2} \cong 1.3$. A similar number was found in experiments with Si(100)-MOSFET structures.¹⁹ We predict that metallic samples at $B=0$ with an electron density given by $N_{\text{MIT}}^{g_s=1} < N < N_{\text{MIT}}^{g_s=2}$ can be made insulating by applying a parallel magnetic field $B > B_c$. Samples with $N > N_{\text{MIT}}^{g_s=1}$ always will stay metallic in a parallel magnetic field and samples with $N < N_{\text{MIT}}^{g_s=2}$ are always insulating, independent of the applied parallel magnetic field.

For a parallel magnetic field we predict in Fig. 3 the mag-

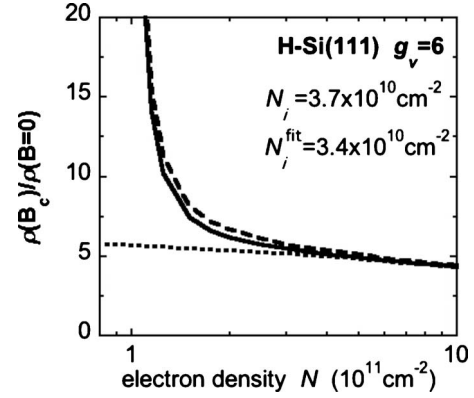


FIG. 3. Magnetoresistance ratio $\rho(B_c)/\rho(B=0)$ versus electron density N of the two-dimensional electron gas for charged-impurity scattering at the H-Si(111) interface with $N_i = 3.7 \times 10^{10} \text{ cm}^{-2}$. For the solid line multiple-scattering effects are taken into account. The dotted line represents the lowest order result $\mu_0(g_s=2)/\mu_0(g_s=1)$. The dashed line represents the calculation using the analytical formula $\mu_{\text{fit}}(g_s=2)/\mu_{\text{fit}}(g_s=1)$ with $N_i^{\text{fit}} = 3.4 \times 10^{10} \text{ cm}^{-2}$.

netoresistance ratio $\rho(B=B_c)/\rho(B=0) \equiv \mu(g_s=2)/\mu(g_s=1)$ versus electron density for charged-impurity scattering. For the dotted line in Fig. 3 MSE are neglected, which corresponds to $\mu_0(g_s=2)/\mu_0(g_s=1)$.

The dashed line is obtained using $\mu_{\text{fit}}(g_s=2)/\mu_{\text{fit}}(g_s=1)$. For $N \gg N_{\text{MIT}}^{g_s=1} \approx 7.94 \times 10^{10} \text{ cm}^{-2}$ and for $g_v = 6$ one finds for the ratio $\rho(B=B_c)/\rho(B=0) \approx 5$, a ratio much larger than for silicon (100) with $g_v = 2$, where a ratio $\rho(B=B_c)/\rho(B=0) \approx 2.5$ is found in experiment.²¹ We believe that the divergent behavior of the magnetoresistance ratio at $N_{\text{MIT}}^{g_s=1}$ can be studied in detail when the electron density of a sample can be modified by a gate.

The temperature dependence of the mobility, according to Eq. (3), is given by the coefficient $C(\alpha, N)$. The coefficient $C(-1, N)$ for charged-impurity scattering as function of the electron density is shown in Fig. 4 as the solid line according

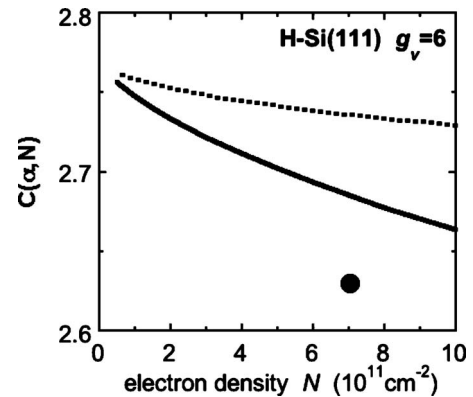


FIG. 4. Coefficient $C(\alpha, N)$ for the temperature dependence of the mobility versus electron density N of the two-dimensional electron gas at the H-Si(111) interface for charged-impurity scattering ($\alpha = -1$) as the solid line. The dotted line represents the ideal 2DEG with $\delta(z)$ confinement within the RPA and charged-impurity scattering. The solid dot represents a result calculated from experimental data given in Ref. 7.

to Ref. 25. We note that $C(-1, N)$ is only weakly density dependent and roughly given by $C(-1, N) = 4 \ln 2 \approx 2.8$. This is the result of the large valley degeneracy, where the ratio $2k_F/q_s \propto 1/g_v^{3/2}$ is very small in the density range shown. q_s represents the screening wave number $q_s = g_s g_v / a^* = 12/a^*$. $2k_F/q_s \ll 1$ is the reason why many-body effects, described by the LFC, nearly cancel out for H-Si(111) in the measured density range, see Eq. (26b) in Ref. 25. The dotted line in Fig. 4 represents the ideal 2DEG of zero width where many-body effects are neglected. For Si(111) the difference between the two results is small. The solid dot in Fig. 4 represents an experimental result calculated from Fig. 2b of Ref. 7: $C(\alpha, N = 7.02 \times 10^{11} \text{ cm}^{-2}) = 2.63$. $N = 7.02 \times 10^{11} \text{ cm}^{-2}$ is high enough for the lowest order result μ_0 being a reasonable description of the experimental mobility. Reasonable agreement between theory and experiment is seen. However, it should be noted that the experimental results in Ref. 7 are shown in a log/log plot. This is not a good way to see the linear temperature dependence.

We stress that the temperature dependence in Eq. (3) is based on the lowest order result μ_0 , which cannot describe the mobility at zero temperature at electron densities near the MIT, see Fig. 1. We believe that the temperature dependent experimental results obtained in Ref. 7 are interesting in connection with the temperature dependence of the mobility near the MIT, which cannot be described by the lowest order result. The numerical results of the mobility obtained for different temperatures in Ref. 26 cannot describe the experiments: the reason is that the lowest order result of the mobility cannot be used near the MIT, see Fig. 1.

We claim that the calculated mobility, including MSE, is in surprising good agreement with the experimental results, see Fig. 1. We noted this good agreement already before when comparing the mode-coupling theory with experiments. In these earlier experiments discussed in Refs. 12 and 13 the peak mobility was relatively low $\mu_{peak} \leq 2 \times 10^4 \text{ cm}^2/\text{Vs}$. For GaAs/AlGaAs heterostructures with higher mobility, discussed in Ref. 17, an additional parameter, the remote doping distance, was used. For the high mobility sample of Ref. 7 and discussed in this paper the disorder is small. We consider the agreement between theory and experiment for this high mobility sample as a large progress from a theoretical point of view: only one scattering mechanism is involved and characterized by one number, the impurity density. Many-body effects for the strongly correlated electron liquid via the LFC have been taken into account. We assumed that the impurities are at the interface vacuum/

Si(111). We believe that in the H-Si(111) samples the impurity density can be modified experimentally, using hydrogen. Therefore, we expect to see in the near future samples with different mobility, depending on N_i . We expect that a 2DEG with ultra-high mobility can be produced on the surface of H-Si(100).

The MIT obtained in the mode-coupling approach¹³ represents a disorder-induced quantum-phase transition, occurring at zero temperature by varying the electron density for given impurity density (or varying the impurity density for given electron density). This MIT also exist in the 2DEG at Si(100) interface,^{1,12,13,22} as well as in GaAs/AlGaAs heterostructures.^{17,19} This disorder induced MIT is an Anderson transition, however, in a system where interaction effects are present and important and enter the theory as a screening effect where non-trivial many-body effects are important.

Recent experimental results concerning the MIT in the 2DEG and reviewed in Ref. 19 mainly concern an interaction induced MIT, believed to be driven by a divergent effective mass. It was claimed, using strongly disordered Si(111) MOSFET structures with $g_v = 2$, that this interaction induced MIT is universal and occurs at $r_s^* \approx 9.3$.⁴ For H-Si(111) this r_s^* value would correspond to $N^* \approx 4.3 \times 10^{11} \text{ cm}^{-2}$. In H-Si(111) the effective mass as function of the electron density was not yet measured. However, it seems that nothing special in the transport data of Ref. 7 is seen near $N^* \approx 4.3 \times 10^{11} \text{ cm}^{-2}$. In addition, it is still unclear what could be the origin of this diverging mass apparently observed in Si(100) and Si(111) MOSFET structures. We stress that it was shown that the published transport data of the Si(111) system can be explained by the mode-coupling theory by using a diverging effective mass as input in the theory.⁸

In conclusion we have shown that the recently measured mobility⁷ of the two-dimensional electron gas in H-Si(111) can be interpreted by charged impurities located at the vacuum/silicon interface with an impurity concentration $N_i = 3.7 \times 10^{10} \text{ cm}^{-2}$. Our transport theory, including multiple-scattering effects and many-body effects, describes the data with a metal-insulator transition at $N_{MIT} = 7.94 \times 10^{10} \text{ cm}^{-2}$. We calculated the transport properties of the fully spin-polarized electron gas, including the metal-insulator transition for the spin-polarized system, which can be tested in experiment. We predict that the resistance ratio $\rho(B_c)/\rho(B=0) \approx 5$ in Si(111) with $g_v = 6$ is strongly increased compared to Si(100) with $g_v = 2$. Analytical results for the mobility are presented and are shown to be very useful in comparison with experiments.

¹T. Ando, A. B. Fowler, and F. Stern, *Rev. Mod. Phys.* **54**, 437 (1982).

²D. C. Tsui and G. Kaminsky, *Phys. Rev. Lett.* **42**, 595 (1979).

³O. Estibals, Z. D. Kvon, G. M. Gusev, G. Arnaud, and J. C. Portal, *Physica E* **22**, 446 (2004).

⁴A. A. Shashkin, A. A. Kapustin, E. V. Deviatov, V. T. Dolgoplov, and Z. D. Kvon, *Phys. Rev. B* **76**, 241302(R) (2007).

⁵K. Eng, R. N. McFarland, and B. E. Kane, *Appl. Phys. Lett.* **87**,

052106 (2005).

⁶K. Eng, R. N. McFarland, and B. E. Kane, *Phys. Rev. Lett.* **99**, 016801 (2007).

⁷R. N. McFarland, T. M. Kott, L. Sun, K. Eng, and B. E. Kane, *Phys. Rev. B* **80**, 161310(R) (2009).

⁸A. Gold, *J. Phys.: Condens. Matter* **19**, 506214 (2007).

⁹A. Gold and O. Antonie, *Int. J. Mod. Phys. B* **21**, 1529 (2007).

¹⁰A. Gold, L. Fabie, and V. T. Dolgoplov, *Appl. Phys. Lett.* **91**,

- 052112 (2007); *Physica E* **40**, 1351 (2008).
- ¹¹The MIT should be defined by extrapolating the temperature-dependent mobility to zero temperature and not by $d\mu(T)/dT \equiv 0$.
- ¹²A. Gold, *Phys. Rev. Lett.* **54**, 1079 (1985).
- ¹³A. Gold and W. Götze, *Phys. Rev. B* **33**, 2495 (1986).
- ¹⁴D. Pines and P. Nozières, *The Theory of Quantum Liquids* (Benjamin, New York, 1966), Vol. 1.
- ¹⁵K. S. Singwi and M. P. Tosi, *Solid State Phys.* **36**, 177 (1981).
- ¹⁶A. Gold and L. Calmels, *Phys. Rev. B* **48**, 11622 (1993); A. Gold, *ibid.* **50**, 4297 (1994); *Z. Phys. B* **103**, 491 (1997).
- ¹⁷A. Gold, *Phys. Rev. B* **44**, 8818 (1991).
- ¹⁸M. Rahimi, S. Anissimova, M. R. Sakr, S. V. Kravchenko, and T. M. Klapwijk, *Phys. Rev. Lett.* **91**, 116402 (2003).
- ¹⁹S. V. Kravchenko and M. P. Sarachik, *Rep. Prog. Phys.* **67**, 1 (2004).
- ²⁰T. Okamoto, K. Hosoya, S. Kawaji, and A. Yagi, *Phys. Rev. Lett.* **82**, 3875 (1999).
- ²¹V. T. Dolgoplov and A. Gold, *JETP Lett.* **71**, 27 (2000); A. Gold and V. T. Dolgoplov, *Physica E* **17**, 280 (2003).
- ²²A. Gold, *JETP Lett.* **72**, 274 (2000).
- ²³F. Stern, *Phys. Rev. Lett.* **44**, 1469 (1980).
- ²⁴A. Gold and V. T. Dolgoplov, *J. Phys. C* **18**, L463 (1985).
- ²⁵A. Gold and V. T. Dolgoplov, *Phys. Rev. B* **33**, 1076 (1986).
- ²⁶E. H. Hwang and S. Das Sarma, *Phys. Rev. B* **75**, 073301 (2007).